

This is a self-archived version of an original article. This version may differ from the original in pagination and typographic details.

Author(s): Kusić, Denis; Connolly, Joanne; Kainulainen, Heikki; Semenova, Ekaterina A.; Borisov, Oleg V.; Larin, Andrey K.; Popov, Daniil V.; Generozov, Edward V.; Ahmetov, Ildus I.; Britton, Steve L.; Koch, Lauren G.; Burniston, Jatin G.

Title: Striated muscle-specific serine/threonine-protein kinase beta (SPEG β) segregates with high- versus low-responsiveness to endurance exercise training

Year: 2020

Version: Accepted version (Final draft)

Copyright: © 2019, Physiological Genomics

Rights: In Copyright

Rights url: <http://rightsstatements.org/page/InC/1.0/?language=en>

Please cite the original version:

Kusić, D., Connolly, J., Kainulainen, H., Semenova, E. A., Borisov, O. V., Larin, A. K., Popov, D. V., Generozov, E. V., Ahmetov, I. I., Britton, S. L., Koch, L. G., & Burniston, J. G. (2020). Striated muscle-specific serine/threonine-protein kinase beta (SPEG β) segregates with high- versus low-responsiveness to endurance exercise training. *Physiological Genomics*, 52(1), 35-46.
<https://doi.org/10.1152/physiolgenomics.00103.2019>

1 **Striated muscle-specific serine/threonine-protein kinase beta (SPEG β) segregates with**
2 **high- versus low-responsiveness to endurance exercise training**

3 **Running Head: SPEG β segregates with responsiveness to endurance training**

4
5 Denis Kusić¹, Joanne Connolly³, Heikki Kainulainen⁴, Ekaterina A. Semenova⁵, Oleg V. Borisov^{5,6}, Andrey K.
6 Larin⁵, Daniil V. Popov⁷, Edward V. Generozov⁵, Ildus I. Ahmetov^{1,5,8}, Steven L. Britton^{9,10}, Lauren G. Koch¹¹
7 and Jatin G. Burniston^{1,2†}.

8
9 ¹Research Institute for Sport and Exercise Sciences, ²Liverpool Centre for Cardiovascular Science, Liverpool
10 John Moores University, Liverpool, UK. ³Waters Ltd, Wilmslow, Manchester, UK. ⁴Faculty of Sport and Health
11 Sciences, University of Jyväskylä, Jyväskylä, Finland. ⁵Department of Molecular Biology and Genetics, Federal
12 Research and Clinical Center of Physical-Chemical Medicine of Federal Medical Biological Agency, Moscow,
13 Russia. ⁶Institute for Genomic Statistics and Bioinformatics, University Hospital Bonn, Bonn, Germany.
14 ⁷Laboratory of Exercise Physiology, Institute of Biomedical Problems of the Russian Academy of Sciences,
15 Moscow, Russia. ⁸Laboratory of Molecular Genetics, Kazan State Medical University, Kazan, Russia.
16 ⁹Department of Anaesthesiology, University of Michigan, Ann Arbor, MI, USA. ¹⁰Department of Molecular &
17 Integrative Physiology, University of Michigan, Ann Arbor, MI, USA. ¹¹Department of Physiology and
18 Pharmacology, The University of Toledo, Toledo, OH, USA.

19
20 †Address for Correspondence: Jatin G Burniston PhD FECSS
21 ORCID: 0000-0001-7303-9318
22 Professor of Muscle Proteomics
23 Research Institute for Sport & Exercise Sciences
24 Liverpool Centre for Cardiovascular Science
25 Liverpool John Moores University,
26 Tom Reilly Building, Byrom Street,
27 Liverpool, L3 3AF,
28 United Kingdom.
29 Tel: +44 (0) 151 904 6265
30 Email: j.burniston@ljmu.ac.uk

31 **Keywords:**

32 Artificial selection model; Co-immunoprecipitation; Endurance training; Exercise capacity; Label-free
33 quantitation; Liquid chromatography mass spectrometry; Responsiveness to exercise; Skeletal muscle.

35 **Supplementary data.**

36 <https://doi.org/10.6084/m9.figshare.9995087> (<https://figshare.com/s/1684cf1d68caa238fddb>)

37 **Abstract**

38 Bi-directional selection for either high- or low-responsiveness to endurance running has created divergent
39 rat phenotypes of high-response trainers (HRT) and low-response trainers (LRT). We conducted proteome
40 profiling of HRT and LRT gastrocnemius of 10 female rats (body weight 279 ± 35 g; n=5 LRT and n=5 HRT)
41 from generation 8 of selection. Differential analysis of soluble proteins from gastrocnemius was conducted
42 using label-free quantitation. Genetic association studies were conducted in 384 Russian international-level
43 athletes (age 23.8 ± 3.4 y; 202 males and 182 females) stratified to endurance or power disciplines.
44 Proteomic analysis encompassed 1,024 proteins, 76 of which exhibited statistically significant ($P < 0.05$, FDR
45 $< 1\%$) differences between HRT and LRT muscle. There was significant enrichment of enzymes involved in
46 glycolysis/ gluconeogenesis in LRT muscle but no enrichment of gene ontology phrases in HRT muscle.
47 Striated muscle-specific serine/threonine-protein kinase beta (SPEG β) exhibited the greatest difference in
48 abundance and was 2.64-fold greater ($P = 0.0014$) in HRT muscle. Co-immunoprecipitation identified 24
49 potential binding partners of SPEG β in HRT muscle. The frequency of the G variant of the rs7564856
50 polymorphism that increases *SPEG* gene expression, was significantly greater (32.9 vs 23.8%; OR = 1.6, $P =$
51 0.009) in international-level endurance athletes (n=258) compared to power athletes (n=126) and was
52 significantly associated ($\beta = 8.345$, $P = 0.0048$) with a greater proportion of slow-twitch fibres in vastus
53 lateralis of female endurance athletes. Co-immunoprecipitation of SPEG β in HRT muscle discovered putative
54 interacting proteins that link with previously reported differences in transforming growth factor- β signalling
55 in exercised muscle.

56

57 Introduction

58 Exercise training has a positive impact on health and is broadly considered to be effective in the prevention
59 of chronic diseases, including type 2 diabetes mellitus and cardiovascular disease (56). In humans, maximum
60 aerobic capacity ($VO_2\text{max}$) is a strong and independent indicator of mortality (40), and also modifies risk
61 associated with factors collectively termed the metabolic syndrome, including insulin resistance, abdominal
62 obesity, atherogenic dyslipidaemia, hypertension, and a proinflammatory and prothrombotic state (16). An
63 individual's $VO_2\text{max}$ is a product of their genetic heritage as well as their recent history of habitual activity or
64 exercise training. However, there is broad inter-individual variation in the response of humans to exercise
65 training (5, 22). The Health, Risk Factors, Exercise Training and Genetics (HERITAGE) family study reported
66 47 % of the variance in responsiveness (improvement in $VO_2\text{max}$) to training may be attributable to genetic
67 and other familial factors (4). In Caucasian men and women, the average increase in $VO_2\text{max}$ after 20-weeks
68 supervised training, was 400 ml/min, but the magnitude of improvement in $VO_2\text{max}$ was broadly distributed,
69 for example the $VO_2\text{max}$ of some individuals increased by more than 1,000 ml/min (relative increase of
70 approximately 50 %). In contrast, other individuals failed to show a measurable change in $VO_2\text{max}$ or
71 responded negatively and exhibited a decrease in $VO_2\text{max}$ in response to the standardised exercise stimulus.
72 Moreover, changes in insulin sensitivity varied widely and 42 % of the 596 HERITAGE participants that
73 underwent an intravenous glucose tolerance test exhibited no change or a decrease in insulin sensitivity
74 after exercise training (7). Such an inability to respond to aerobic exercise may have serious health
75 consequences and investigation of the mechanisms underpinning this phenomenon is needed to identify
76 targets and candidate biomarkers for more personalised therapies.

77 In humans a mixture of genetic and environmental factors contribute to the broad range of responsiveness
78 to exercise training and this presents challenges to identifying the underlying mechanistic links between
79 exercise and improvements in health outcomes. The genetic factors that contribute to $VO_2\text{max}$ (and
80 therefore disease risk) interact with environment factors and can be divided into intrinsic and acquired
81 components. The intrinsic component governs an individual's baseline aerobic capacity and disease
82 risk-profile in the non-trained sedentary state, whereas the acquired component governs the individual's
83 responsiveness to an environment of high physical-activity such as regular endurance training. The intrinsic
84 and acquired components of exercise capacity are each selectable traits and we have used bi-directional
85 artificial selection in rats to develop models of either high- versus low-intrinsic running capacity or high-
86 versus low-responsiveness to endurance training. Selection on intrinsic running capacity has generated
87 high-capacity runners (HCR) that resemble endurance-trained individuals and low-capacity runners (LCR)
88 that have a significantly heightened disease risk profile, including significantly poorer cardiovascular function
89 (e.g. (57)), peripheral insulin sensitivity (e.g. (47)) and life expectancy (e.g. (30)). Selection on the acquired
90 component of exercise capacity has generated high-response to training (HRT) and low-response to training
91 (LRT) rats (31, 48) that do not differ in their intrinsic running capacity but have significantly different

92 responses to a standardised regimen of endurance training. After 8 weeks of moderate endurance exercise,
93 the maximal running capacity of HRT rats increases by on average 50 %, whereas LRT rats either fail to
94 respond positively or decrease in maximal running capacity on average by 50 %. Lessard et al (33) reports
95 LRT exhibit primary metabolic defects including poor glucose tolerance and elevated plasma triacylglyceride
96 levels in the untrained sedentary state, and when exposed to endurance training LRT fail to promote skeletal
97 muscle angiogenesis and exhibit an altered inflammatory response to acute exercise. It is not yet clear
98 whether common molecular targets from hypothesis-led literature on muscle responses to exercise training
99 are differentially regulated in HRT/LRT muscle. For example, Lessard et al (33) reports no difference in the
100 response of signalling proteins (e.g. AMPK and Akt) or mitochondrial capacity between HRT/LRT rats exposed
101 to exercise training. In contrast, Marton et al (37) conclude there are significant differences in markers of
102 mitochondrial biogenesis in the muscles HRT and LRT rats exposed to controlled exercise training.

103 Wider analysis of molecular differences that regress with low- versus high-responsiveness to endurance
104 training may provide further mechanistic insight to the regulators of the training response and the elevated
105 disease risk that is associated with a lack of adaptation to endurance training. Nevertheless, finding the
106 common denominators that underpin differences in the change in exercise capacity in response to
107 endurance training is challenging because the genetic underpinning of training responsiveness is highly
108 convoluted. Previous attempts to find predictors of exercise responsiveness have been performed at the
109 transcript level, which offers powerful bioinformatic analysis through reverse engineering of nucleotide data
110 and has highlighted complex relationships such as the repression of negative regulators (e.g. miRNA) that
111 target selective transcription factors (28). Proteomic analysis offers an alternative and pragmatic approach
112 to discovering new information that may be complementary to other omic approaches (59), and we (9, 10)
113 have previously used proteomics to highlight differences in HCR/LCR muscle that segregate with intrinsic
114 running capacity. The proteome/ protein complement of a tissue is what defines that tissue and is the net
115 result of complex upstream events involving genetic and environmental interactions. The proteome is often
116 regarded as a product downstream of transcriptional processing, translational regulation and protein
117 degradative processes. However, proteins that already exist within the cell are what 'sense' and transduce
118 environmental stimuli, and so also reside upstream of gene transcription and other regulatory processes. To
119 gain new insight to muscle proteome differences associated with the responsiveness to endurance training,
120 we conducted high-definition mass spectrometry (HDMS^E; (8)) profiling of proteins in HRT and LRT
121 gastrocnemius. We report comprehensive differences between HRT and LRT muscle, including a greater
122 abundance of straited muscle-specific serine/threonine protein kinase beta (SPEG β) in HRT gastrocnemius.
123 We identify putative binding partners of SPEG β in rat muscle that link with previously reported differences in
124 transforming growth factor- β (TGF- β) signalling. Moreover, genetic analysis in international-level Russian
125 athletes found the G variant of the rs7564856 polymorphism that increases *SPEG* gene expression, was
126 significantly greater in endurance than power athletes, which offers some external validation of the potential
127 role of SPEG β in modulating muscle responsiveness to endurance training.

129 **Methods**

130 **Rat model of artificial selection on responsiveness to endurance exercise training.**

131 High-response trainer (HRT) and low-response trainer (LRT) rats were generated from a large-scale
132 bi-directional selection programme on the response to endurance exercise described in Koch et al (31).
133 Briefly, genetically heterogeneous rats (n= 152) from the N:NIH outcrossed stock were used to develop the
134 HRT and LRT strains by selective mating of males and females that exhibited either the greatest (HRT) or
135 least (LRT) response (improvement in exercise capacity) to a standardised and progressive regimen of
136 endurance training. The maximal running capacity (maximum distance run; DIST) of each animal was
137 measured using a speed-ramped treadmill test to exhaustion that was performed prior to (DIST1) and after
138 (DIST2) an 8-week programme of 24 exercise sessions beginning when the animals were approximately
139 11-13 weeks of age. The volume of endurance training progressed each session by increments of 1 m/min
140 running speed and 0.5 min duration, beginning at 10 m/min for 20 min in the 1st week and finishing at 21
141 m/min for 31.5 min in the 8th week. All exercise tests and training sessions were performed on a motorised
142 treadmill at a 15 ° incline and the response to training was calculated as the change in maximal running
143 distance (Δ DIST = DIST2 - DIST1). At each generation, 10 male and 10 female rats that represented the
144 extremes of training response were bred to develop HRT and LRT strains. Rats used in the current work were
145 females from generation 8 of selection and were shipped from the U.S. to the University of Jyväskylä, Finland,
146 at 10 months of age. The animals were housed in standard conditions (temperature 22 °C, humidity 50 ±
147 10 %, light from 8.00 a.m. to 8.00 p.m.) and had free access to tap water and food pellets (R36; Labfor,
148 Stockholm, Sweden). The study was approved by the National Animal Experiment Board, Finland (Permit
149 number ESLH-2007-06894/Ym-23) and at the age of 17 months the maximal running capacity of the rats was
150 tested according to the speed-ramped protocol used previously at the University of Michigan. Two weeks
151 after the maximal running test 5 LRT and 5 HRT rats (body mass 290 ± 30 g and 268 ± 40 g, respectively)
152 were euthanized and gastrocnemius muscles were excised, snap-frozen in liquid nitrogen and stored at
153 -80 °C before being shipped to Liverpool John Moores University, UK, for proteomic analysis.

154 **Processing of rat muscle samples**

155 Muscles were pulverised in liquid nitrogen then homogenised on ice in 8 volumes of 1 % NP-40, 50 mM Tris
156 pH 7.4 containing Complete™ protease inhibitor (Roche Diagnostics, Lewes, UK). Samples were incubated on
157 ice for 15 min then centrifuged at 1,000 rpm, 4 °C for 5 min. Supernatants were cleared by centrifugation
158 (12,000 g, 4 °C for 45 min) and protein concentrations were measured using the Bradford assay (Sigma,
159 Poole, Dorset, UK). Each sample was adjusted to 5 µg/µl and in-solution tryptic digestion was performed in
160 preparation for label-free quantitation (LFQ). Aliquots containing 100 µg protein were precipitated in 5
161 volumes of acetone for 1 h at -20 °C. Pellets were resuspended in 0.1 % (w/v) Rapigest SF (Waters; Milford,
162 MA) in 50 mM ammonium bicarbonate and incubated at 80 °C for 15 min. DTT was added (final

163 concentration 1 mM) and incubated at 60 °C for 15 min followed by incubation whilst protected from light in
164 the presence of 5 mM iodoacetamide at 4 °C. Sequencing grade trypsin (Promega; Madison, WI) was added
165 at an enzyme to protein ratio of 1:50 and digestion allowed to proceed at 37 °C overnight. Digestion was
166 terminated by the addition of 2 µl concentrated TFA and peptide solutions were cleared by centrifugation at
167 13 000 g for 15 min. Samples were diluted 1:1 with a tryptic digest of yeast alcohol dehydrogenase 1 (100
168 fmol/ µl) to enable the amount of each identified protein to be quantified, as described previously (51).

169 **Label-free quantitation (LFQ) by high-definition – mass spectrometry (HDMS^E)**

170 Peptide mixtures were analysed by nanoscale reverse-phase ultra-performance liquid chromatography
171 (UPLC; nanoACQUITY, Waters, Milford, MA) and online ion-mobility mass spectrometry (IMS; SYNAPT G2-S,
172 Waters, Manchester, UK). Samples (200 ng tryptic peptides) were loaded in aqueous 0.1 % (v/v) formic acid
173 via a Symmetry C₁₈ 5 µm, 2 cm x 180 µm trap column (Waters, Milford, MA). Separation was conducted at
174 35 °C through an HSS T3 C₁₈ 1.8 µm, 25 cm x 75 µm analytical column (Waters, Milford, MA). Peptides were
175 eluted using a gradient rising to 40 % acetonitrile 0.1 % (v/v) formic acid over 90 min at a flow rate of 300
176 nl/min. Additionally, a Lockmass reference (100 fmol/ µl Glu-1-fibrinopeptide B) was delivered to the
177 NanoLockSpray source of the mass spectrometer at a flow rate of 500 nl/ min, and was sampled at 60 s
178 intervals. For all measurements, the mass spectrometer was operated in a positive electrospray ionisation
179 mode at a resolution of >25,000 FWHM. Prior to analysis, the time of flight analyser was calibrated with a
180 NaCl mixture from m/z 50 to 1990. HDMS^E analyses were conducted within the Tri-wave ion guide.
181 Accumulated ions were separated according to their drift time characteristics in the N₂ gas-filled mobility cell
182 prior to collision induced dissociation (CID) alternating between low (4 eV) and elevated (14-40 eV) collision
183 energies at a scan speed of 0.9 s per function over 50-2000 m/z. Analytical data were LockMass corrected
184 post-acquisition using the doubly charged monoisotopic ion of the Glu-1-fibrinopeptide B. Charge reduction
185 and deconvolution of potential parent-fragment correlation was achieved in the first instance by means of
186 retention and drift time alignment, as described previously (35).

187 HDMS^E spectra were aligned using Progenesis Q1 for Proteomics (Q1-P; Nonlinear Dynamics, Newcastle, UK).
188 Prominent ion features (approximately 1200 per chromatogram) were used as vectors to match each
189 dataset to a common reference chromatogram. An analysis window of 10 min - 100 min and 50 m/z - 1650
190 m/z was selected, which encompassed a total of 47,109 features (charge states of +2, +3 or +4) and 3,924 of
191 these features were separated by IMS. Protein identifications and quantitative information were extracted
192 using the dedicated algorithms in ProteinLynx GlobalSERVER (PLGS) v3.0 (Waters, Milford, MA). Peak lists
193 were searched against the UniProt database restricted to 'Rattus' (8,071 entries). The initial ion-matching
194 requirements were ≥ 1 fragment per peptide, ≥ 3 fragments per protein and ≥ 1 peptide per protein. The
195 enzyme specificity was trypsin allowing 1 missed cleavage, carbamidomethyl of cysteine (fixed) and oxidation
196 of methionine (variable). Parent- and fragment-ion ppm errors were calculated empirically and decoy
197 databases were used to calculate the identification error rate. Scoring of the database searches was refined

198 by correlation of physicochemical properties of fragmented peptides from theoretical and experimental data.
199 Peptide identifications were imported to QI-P and filtered to exclude peptides with scores less than 5.5 (34).
200 In total, 16, 749 peptides were identified and 1,018 had been resolved by IMS.

201 **Co-IP and GeLC-MS/MS**

202 Co-immunoprecipitation (Co-IP) experiments were performed using a rabbit anti-SPEG polyclonal Ab
203 (HPA018904; Sigma-Aldrich, Poole, Dorset, UK). Negative control Co-IP experiments were conducted using
204 rabbit anti-NDRG2 monoclonal Ab (Ab174850; Abcam plc) or by incubating samples with Protein-A
205 Dynabeads (Thermoscientific, Runcorn, UK) only. Protein A dynabeads were suspended in
206 phosphate-buffered saline with 0.05 % Tween-20 (PBS-T) and rotated for 30 min at room temperature with 1
207 µg of polyclonal antibody in 50 µl of PBS-T. The bead-antibody complex was washed five times in 50 µl of
208 PBS-T and incubated with 500 µg of muscle protein for 3 h at 4 °C on sample mixer. The bead-Ab-sample
209 complexes were washed 3 times in PBS-T, and proteins were extracted from the beads by two sequential
210 incubations in 5 µl of LDS sample buffer (NuPAGE; Thermo Scientific, Runcorn, UK) for 4 min each at 95 °C.
211 Samples were electrophoresed through 7 % Tris-Acetate pre-cast gels (NuPAGE; Thermo Scientific, Runcorn,
212 UK) and stained for 1 h with Colloidal Coomassie blue (BioRad, Deeside, UK). Each gel lane was cut into 7 x 5
213 mm segments and each segment was diced in to 1 mm³ pieces and tryptic in-gel digestion was performed as
214 described previously (20). Each segment was processed separately in preparation for nanoscale
215 reverse-phase UPLC (NanoAcquity; Waters, Milford, MA) and online ESI QTOF MS/MS (Q-TOF Premier;
216 Waters, Manchester, UK). Peptides were desalted using C₁₈ ZipTips (Millipore, Billerica, MA, USA) and loaded
217 by partial-loop injection on to a 180 µm ID x 2 cm long 100 Å, 5 µm BEH C₁₈ Symmetry trap column (Waters,
218 Milford, MA) at flow rate of 5 µl/min for 3 min in 2.5 % (v/v) ACN, 0.1% (v/v) FA. Separation was conducted
219 at 35 °C via a 75 µm ID x 25 cm long 130 Å, 1.7 µm BEH C₁₈ analytical reverse-phase column (Waters, Milford,
220 MA). Peptides were eluted using a linear gradient that rose to 37.5 % ACN 0.1% (v/v) FA over 90 min at a
221 flow rate of 300 nl/min. Eluted peptides were sprayed directly in to the MS via a NanoLock Spray source and
222 Picotip emitter (New Objective, Woburn, MA). Additionally, a LockMass reference (100 fmol/µl
223 Glu-1-fibrinopeptide B) was delivered to the NanoLock Spray source of the MS and was sampled at 240 s
224 intervals. For all measurements, the MS was operated in positive ESI mode at a resolution of 10,000 FWHM.
225 Before analysis, the TOF analyser was calibrated using fragment ions of [Glu-1]-fibrinopeptide B from m/z 50
226 to 1990. Peptide MS were recorded between 350 and 1600 m/z. Data-dependent MS/MS spectra were
227 collected over the range 50–2000 m/z. The 5 most abundant precursor ions of charge 2+ 3+ or 4+ were
228 selected for fragmentation using an elevated (20–40 eV) collision energy. A 30-s dynamic exclusion window
229 was used to avoid repeated selection of peptides for MS/MS.

230 MS/MS spectra were searched against the UniProt database restricted to Rattus (8,071 sequences) using
231 Mascot Distiller (www.matrixscience.com) and a locally implemented Mascot server (v.2.2.03;
232 www.matrixscience.com). Enzyme specificity was trypsin (allowing 1 missed cleavage), carbamidomethyl

233 modification of cysteine (fixed), deamidation of asparagine and glutamine (variable), oxidation of methionine
234 (variable) and m/z errors of 0.3 Da.

235 **Genetic association studies in human athletes**

236 Genetic association studies were conducted in 384 Russian international-level athletes that have been
237 reported in previous studies (e.g. (2, 42)). Participants (age 23.8 ± 3.4 y; 202 males and 182 females)
238 included in the current cohort were of Caucasian Eastern European descent and were stratified into 2 groups.
239 Group 1 (n = 258) included endurance athletes (3-10 km runners, biathletes, 5-10 km skaters, cross-country
240 skiers, marathon runners, 0.8-25 km swimmers, rowers/kayakers, race walkers, 1.5-10 km speed skaters and
241 triathletes). Of those, 35 female endurance athletes were also involved in the muscle biopsy study. Group 2
242 (n = 126) comprised power athletes (50-100 m swimmers, sprint cyclers, 100-400 m runners, 500-1000 m
243 speed skaters and short-trackers, track and field jumpers, heptathletes / decathletes, and throwers). The
244 study was approved by the Ethics Committee of the Physiological Section of the Russian National Committee
245 for Biological Ethics and Ethics Committee of the Federal Research and Clinical Center of Physical-chemical
246 Medicine of the Federal Medical and Biological Agency of Russia. Written informed consent was obtained
247 from each participant. The study complied with the guidelines set out in the Declaration of Helsinki and
248 ethical standards in sport and exercise science research.

249 Venous blood samples (4 ml) were collected in EDTA-coated tubes (Vacuette EDTA, Greiner Bio-One, Austria)
250 and were transported to the laboratory at 4 °C. DNA was extracted from leukocytes on the same day using a
251 commercial kit according to the manufacturer's instructions (Technoclon, Russia). DNA quality was assessed
252 by agarose gel electrophoresis and HumanOmni1-Quad BeadChips (Illumina Inc, USA) were used for
253 genotyping of 1,140,419 single nucleotide polymorphisms (SNPs). In addition, Human OmniExpress
254 BeadChips (Illumina Inc, USA) were used for genotyping of > 700,000 SNPs in the 35 female athletes that also
255 gave muscle samples for fiber-type analysis. The assay required 200 ng of DNA sample as input with a
256 concentration of at least 50 ng/ μ l. Exact concentrations of DNA in each sample were measured using a Qubit
257 Fluorometer (Invitrogen, USA). All further procedures were performed according to the instructions of
258 Infinium HD Assay.

259 **Evaluation of muscle fiber composition in human athletes**

260 Samples of the vastus lateralis muscle of 35 female athletes were obtained with the Bergström needle
261 biopsy procedure under local anaesthesia with 1 % lidocaine solution. Serial cross-sections (7 μ m thick) were
262 cut from frozen muscle samples using a microtome (Leica Microsystems, Wetzlar, Germany) and were
263 thaw-mounted on Polysine glass slides. Sections were air-dried for 15 min at RT and then washed in 3 x 5
264 min incubations in PBS before being incubated (RT for 1 h) in PBS containing primary Ab against slow or fast
265 isoforms of myosin heavy chain (M8421, 1:5000; M4276; 1:600, respectively; Sigma-Aldrich, USA). Muscle
266 sections were washed for 3 x 5 min in PBS and then incubated (RT for 1 h) in PBS containing secondary Ab

267 conjugated with FITC (F0257; 1:100; Sigma-Aldrich). Sections were washed in PBS (3 × 5 min), placed in
268 mounting media and covered with a cover slip prior to imaging using a fluorescent microscope (Eclipse Ti-U;
269 Nikon, Japan). All analysed images contained >100 fibers and the ratio of the number of stained fibers to the
270 total fiber number was calculated. Fibers stained in serial sections with antibodies against slow and fast
271 isoforms were considered as hybrid fibers.

272 **Statistical analysis**

273 Data are presented as mean and standard deviation unless otherwise stated. Differences in protein
274 abundance measured by LFQ of LRT and HRT samples (n = 5 in each group) were investigated by one-way
275 analysis of variance, corrected using q-values (53) to a false discovery rate of 1 %. Functional enrichment
276 testing was performed using the Database for Annotation, Visualisation and Integrated Discovery (DAVID;
277 <https://david.ncifcrf.gov>).

278 Genetic variations in or near the human *SPEG* gene were investigated using the Genotype Tissue Expression
279 (GTEx) database (17). Statistical analysis of genotype data was conducted using PLINK v1.90, R (version 3.4.3),
280 and GraphPad InStat (GraphPad Software, Inc., USA) software. Genotype distribution and allele frequencies
281 between athletes in Group 1 or Group 2 were compared using χ^2 tests. Quantitative trait (proportion of
282 slow-twitch muscle fibers) SNP association was tested in a linear additive model. P values < 0.05 were
283 considered statistically significant.

284

285 Results

286 LRT and HRT rats had a maximum running capacity (DIST1) of 852 ± 176 m and 642 ± 98 m, respectively, at
287 ~ 11 weeks of age. After 8 weeks endurance training, the maximum running capacity (DIST2) of LRT ($539 \pm$
288 107 m) had decreased by 49 % (Δ DIST -313 ± 144 m), whereas the maximum running capacity of HRT rats
289 had increased by 44 % (Δ DIST $+376 \pm 111$ m). The running capacity of the animals was retested at 17 months
290 of age and there was no difference between LRT (114 ± 122 m) and HRT (173 ± 102 m) groups.

291 LFQ encompassed 1,024 proteins that were confidently (FDR < 1 %) identified in each of the HRT and LRT
292 samples ($n = 5$, per group). Protein identifications and normalised abundance data are available at
293 <https://doi.org/10.6084/m9.figshare.9995087>. Differential analysis of proteins quantified using three or
294 more peptides revealed the relative abundance of 76 proteins differed significantly ($P < 0.05$, $q < 0.01$)
295 between HRT and LRT groups (Figure 1). Thirteen proteins were more abundant in HRT muscle (Table 1),
296 whereas 63 proteins were more abundant in LRT (Table 2 and Figure 2a). There was significant enrichment
297 of proteins associated with the KEGG metabolic pathways glycolysis and gluconeogenesis in LRT muscle and
298 12 enzymes involved in muscle glycogen/glucose metabolism (Figure 2b) were more abundant compared to
299 HRT muscle. In contrast, there was no significant enrichment of gene ontology phrases or KEGG metabolic
300 pathways amongst the 13 proteins that were more abundant in HRT muscle. The protein most enriched in
301 gastrocnemius of HRT rats was striated muscle-specific serine/threonine-protein kinase beta (SPEG β ; also
302 known as striated muscle preferentially expressed gene). Co-IP GeLC-MS/MS identified 24 potential binding
303 partners of SPEG β in HRT muscle (Table 3). There was no significant enrichment of gene ontology amongst
304 the potential SPEG β binding partners and we were unable to identify binding partners that were specific to
305 either HRT or LRT.

306 Six SNPs (rs13386459, rs907683, rs72965313, rs4674396, rs745027, rs7564856) located in close proximity
307 (i.e. in high linkage disequilibrium) to the *SPEG* gene were significantly ($P < 5 * 10^{-8} - 10^{-13}$) associated with *SPEG*
308 gene expression in human skeletal muscle. Of those, the rs7564856 was available for genotyping in the
309 athletic cohorts using micro-array analysis. According to GTEx data, the G allele of the rs7564856 SNP was
310 reported to be associated ($P = 2.7 * 10^{-8}$) with increased expression of the *SPEG* gene and may be favourable
311 for endurance sports. The G allele of rs7564856 was significantly greater (32.9 vs 23.8%; OR = 1.6, $P = 0.009$)
312 in endurance athletes compared to power athletes (Figure 3). We also found the G allele was significantly (β
313 = 8.345, $P = 0.0048$) associated with increased proportion of slow-twitch muscle fibers in female endurance
314 athletes.

315

316 Discussion

317 We have used robust HDMS^E profiling to compare the abundance of more than 1,000 proteins in
318 gastrocnemius of rats artificially selected (31) as high-responders (HRT) or low-responders (LRT) to
319 endurance training. Stringent differential analysis (P values filtered to 1 % FDR) identified widespread
320 differences that co-segregate with exercise responsiveness and highlighted potential targets for future
321 mechanistic research. SPEG β exhibited the greatest difference in abundance and was 2.64-fold greater in
322 HRT muscle. SPEG β has been highlighted in at least two (18, 43) earlier non-targeted proteomic analyses of
323 acute muscle responses to exercise. In the current work, proteins that co-immunoprecipitated with SPEG β in
324 HRT muscle include novel targets involved in c-Jun N-terminal kinase (JNK) signalling, which has recently
325 emerged as a regulator of the adaptive response of muscle to exercise training (32). In humans, the G allele
326 of SNP rs7564856 near the SPEG β locus was associated with differences in endurance performance and
327 muscle fiber type. These findings provide new insight to the role of SPEG β in muscle and heighten interest in
328 SPEG β as a target for mechanistic research in molecular exercise physiology.

329 Lessard et al (33) reports hyperactivation of JNK in sedentary LRT muscle and alterations to normal TGF- β
330 signalling in response to endurance training. Follow-up analyses (32) found JNK phosphorylates the linker
331 region of similar to mothers against decapentaplegic homolog 2 (SMAD2) and, thereby, inhibits canonical
332 myostatin-TGF β signalling. In human muscle, JNK phosphorylation of the SMAD2 linker region is particularly
333 robust after resistance rather than endurance exercise (32). Phosphorylation of the SMAD2 linker region
334 potentiates muscle adaptation to resistance exercise but activation of JNK in response to endurance exercise
335 (i.e. as in LRT muscle) appears to be an inappropriate response and is associated with blunted adaptation to
336 endurance training (33). The events upstream of exercise-induced phosphorylation of SMAD2 by JNK have
337 not yet been elucidated. Interestingly, several of the proteins that co-immunoprecipitated with SPEG β in HRT
338 muscle (Table 3) are implicated in JNK and TGF β signalling and could represent viable candidates to
339 investigate differences in TGF β -mediated responses to endurance exercise. Caveolin-1 (CAV1)
340 co-immunoprecipitated with SPEG β and a greater expression of CAV1 mRNA was previously highlighted by
341 transcriptome profiling of HRT/LRT muscle (28). CAV1 inhibits TGF β -mediated activation of SMAD2 by
342 promoting degradation of TGF- β receptors (32). Similarly, ventricular zone-expressed PH domain-containing
343 protein homolog 1 (VEPH1) may also interfere with TGF β -targeted signalling by impeding nuclear
344 accumulation of SMAD2 (49). Serine/threonine-protein kinase (TAOK3), which was initially named JNK
345 inhibitory kinase (55), downregulates the activity of JNK (26) and, therefore, may be the most likely of the
346 putative SPEG β interacting partners to play a mechanistic role in modulating muscle adaptation to endurance
347 training.

348 Targeted investigations of SPEG β binding partners in skeletal muscle report SPEG β interacts with
349 myotubularin and co-localises with other proteins of the junctional sarcoplasmic reticulum (SR), including the
350 dihydropyridine receptor, sarcoplasmic/endoplasmic reticulum Ca²⁺-ATPase (SERCA), and the Z-band protein,

351 desmin (1). Accordingly, skeletal muscles of SPEG knockout mice exhibit centronuclear myopathy (1) and
352 deficits in force that are associated with impaired RyR1-mediated Ca^{2+} release from the SR (23). Similar
353 protein-protein interactions also occur in cardiac muscle (46), where SPEG β phosphorylates SERCA2a and
354 promotes SERCA2a oligomerisation, which is associated with enhanced Ca^{2+} transport activity (45). In the
355 current analysis, SERCA2 co-immunoprecipitated in control experiments as well as with SPEG β , and so was
356 removed from the list (Table 3) of putative SPEG β interacting partners. However, dynamin 2 (DNM2) was
357 amongst the putative interaction partners of SPEG β . Overexpression of DNM2 increases resting $[\text{Ca}^{2+}]_i$ and is
358 associated with impaired contractile properties and centronuclear myopathy (14). Valosin-containing protein
359 (VSP, also known as transitional endoplasmic ATPase) belongs to the AAA+ ATPase family and
360 immunoprecipitated with SPEG β . VSP is required for lysosomal network dynamics, and upon its inhibition
361 lysosomal network and autophagy are impaired (25).

362 Pathway analysis of proteins enriched in HRT muscle did not find significant enrichment of functional groups,
363 but manual interrogation of Table 1 reveals the protein list is punctuated by features that are common to
364 exercise-trained muscle. For example, HRT muscle has a greater abundance of the fatty acid translocase
365 (CD36), mitochondrial superoxide dismutase (Mn SOD) and 10 kDa heat shock protein (CH10) that are also
366 more abundant in diaphragm of exercise-trained rats (52). Consistent with these findings, gene expression of
367 CD36 is also greater in HRT muscle (28). However, SPEG was not among the genes annotated on the array
368 used in the previous (28) transcriptomic analysis. Notably, there was no overlap between proteins enriched
369 in HRT muscle and those previously reported (9) to be enriched in the soleus proteome of HCR rats selected
370 for high intrinsic running capacity. This is consistent with the difference in genetic heritability of training
371 responsiveness vs intrinsic capacity in rats (31) and humans (6).

372 HRT muscle had greater abundance of proteins associated with store-operated Ca^{2+} entry (SOCE; (44)),
373 including cGMP-gated cation channel alpha-1 (CNGA1), inositol monophosphatase (IMP), stromal interaction
374 molecule 1 (STIM1) and 1-phosphatidylinositol-4,5-bisphosphate phosphodiesterase gamma-1 (PLCG1).
375 SOCE may assist in maintaining the myoplasmic pool of Ca^{2+} during repeated contractions and in doing so
376 may modulate fatigue (41). STIM1 localises to the longitudinal SR and enables rapid activation (13) of SOCE.
377 Muscles of STIM1-haploinsufficient animals have impaired refilling of internal Ca^{2+} stores when subjected to
378 repeated stimulation, fatigue sooner and achieve smaller tetanic forces. In hepatocytes, PLCG1 can activate
379 SOCE independently of STIM1 (36) but the role of PLCG1 in skeletal muscle has not yet been reported.
380 CNGA1 is activated by SOCE (58) at physiological extracellular concentrations, which enables propagation of
381 Ca^{2+} currents through CNGA1 (15). Maintenance of phosphatidylinositol 4,5-bisphosphate (PIP2) levels by
382 IMP supports both SOCE and Ca^{2+} oscillating signals (3). Ca^{2+} signalling is indeed diversely involved in
383 exercise-related adaptations. Oscillations in, and moderate rises to, $[\text{Ca}^{2+}]_i$ upregulate mitochondrial
384 biogenesis (24) and ATP production (19), whereas a prolonged elevation in $[\text{Ca}^{2+}]_i$ is associated with muscle
385 weakness and atrophy (38). Although speculative, exercise-related perturbations in $[\text{Ca}^{2+}]_i$ in LCR muscle may

386 result in prolonged increase in $[Ca^{2+}]_i$ culminating in negative effects that eventually lead to a
387 low-responsiveness phenotype. Increased $[Ca^{2+}]_i$ results in oligomerisation and overexpression of VDAC1,
388 which leads to the formation of apoptosomes and cell death (27). VDAC1 is 1.27-fold more abundant in LRT
389 and the S100a1 Ca^{2+} -binding protein, which is enriched in slow twitch fibers (12), and was 1.4-fold more
390 abundant in LRT. Accounting for a lesser percentage of slow-twitch fibers in LRT gastrocnemius makes the
391 relative difference per fiber more pronounced.

392 LRT gastrocnemius exhibited pronounced enrichment of enzymes involved in glucose metabolic processes
393 (Figure 2b), which may link with the previously (33) reported difference in myofiber profile between HRT and
394 LRT. In the plantaris of LRT rats, the proportion of type I slow-twitch fibers (7 %) is similar to sedentary
395 Wistar rats (50) but significantly less than in HRT muscle (20 %), whereas no difference in myosin heavy chain
396 (MyHC) type IIa myofiber abundance is observed (33). The current proteomic analysis focused on soluble
397 muscle proteins and it is not possible to report the myofiber profile of HRT/LRT gastrocnemius muscle using
398 the current data. The 1.4-fold greater abundance of sarcoplasmic/endoplasmic reticulum ATPase-1 and
399 parvalbumin in LRT muscle alongside the conspicuous enrichment of glycolytic enzymes may suggest a faster
400 twitch myofiber profile in LRT compared to HRT gastrocnemius. However, some mitochondrial proteins were
401 also more abundant in LRT compared to HRT muscle (Table 2).

402 A potential difference in myofiber profile between HRT/LRT gastrocnemius raises the question of whether
403 differences in SPEG β protein abundance may also be a consequence of a difference in MyHC profile. Drexler
404 et al (12) reports comparative proteome analysis of mouse fast-twitch extensor digitorum longus (EDL) and
405 slow-twitch soleus and reports SPEG β amongst those proteins enriched in EDL. Murgia et al (39) reports
406 deep proteome analysis of individual myofibers extracted from vastus lateralis of younger and older human
407 adults. We extracted SPEG β abundance data from Murgia et al (39) and investigated differences due to
408 either MyHC fiber type or age using 2-way analysis of variance. The abundance of SPEG β was not different
409 ($P=0.8144$) between muscles of younger and older adults, but SPEG β abundance was significantly ($P=0.0288$)
410 different across different myofiber types. SPEG β abundance was 65 % greater ($P=0.0129$) in MyHC IIx than
411 type I fibers while fibers containing MyHC IIa were intermediate and SPEG β abundance was 21 % greater
412 ($P=0.7463$) in MyHC IIa containing fibers compared to MyHC type I (Tukey HSD post-hoc analysis). Therefore,
413 potential differences in myofiber profile between HRT and LRT gastrocnemius seem to be an unlikely
414 explanation for the greater abundance of SPEG β in HRT muscle.

415 SPEG β is serine/threonine protein kinase homologous to proteins of the myosin light chain kinase family (54).
416 In C2C12 myoblasts, expression of the alpha isoform of SPEG co-occurs with myoblast differentiation and the
417 emergence of myosin heavy chain expression (21). Whereas, SPEG β is solely detected in adult muscle *in vivo*
418 (21), suggesting expression of the beta isoform may be instigated during postnatal maturation in response to
419 contractile activity. SPEG β is a phosphoprotein and we (18) reported greater phosphorylation of SPEG β in rat
420 heart 0-3 h after an incremental exercise test to VO_{2max} . Similarly, Potts et al (43) reports phosphorylation

421 of SPEG β occurs in mouse skeletal muscle 1 h after a protocol of maximal-intensity contractions. In the
422 current work, the abundance of SPEG β is greater (2.64-fold, $P=0.0014$) in gastrocnemius of rats that exhibit
423 high-responsiveness to endurance training. Although we did not investigate the phosphorylation status of
424 SPEG β in HRT/LRT gastrocnemius, the evidence to date suggests SPEG β functions as a mechanosensitive
425 kinase in striated muscle. In the future, it would be interesting to investigate whether either SPEG β
426 abundance or phosphorylation status changes in response to long-term endurance training. We were unable
427 to find data reporting SPEG β abundance in trained versus untrained muscle, but we did identify that the
428 frequency of the G variant of SNP rs7564856 (that increases the expression of the SPEG gene) is greater in
429 endurance compared to power athletes. The G allele of SNP rs7564856 was also significantly associated with
430 increased proportion of slow-twitch muscle fibers in female endurance athletes. In addition, in 130,000 UK
431 Biobank participants, rs7564856 is associated ($P=1.63 \times 10^{-11}$) with the pulmonary ratio of forced expiratory
432 volume in the first one second (FEV1)/ forced vital capacity (FVC) (29), which is a surrogate indicator of
433 $VO_2\max$ (11).

434 In conclusion, artificial selection for high responsiveness to endurance training is associated with a greater
435 abundance of SPEG β in rat gastrocnemius. Co-immunoprecipitation of SPEG β in HRT muscle discovered
436 putative interacting proteins that may link with previously reported differences in TGF β signalling in
437 exercised muscle. In humans, genetic polymorphisms near the *SPEG* gene locus are associated with higher
438 expression of SPEG β , which may favour endurance phenotypes. These findings alongside recent reports of
439 acute phosphorylation of SPEG β in cardiac (18) and skeletal muscle (43) in response to acute exercise
440 support the hypothesis that SPEG β is an important component in the adaptational response of muscle to
441 exercise and warrants further mechanistic study.

442 **Acknowledgements**

443 The exercise rat models are funded by the Office of Research Infrastructure Programs grant P40OD021331
444 from the National Institutes of Health. The rat models for low and high exercise response to training are
445 maintained as an international resource with support from the Department of Physiology & Pharmacology,
446 University of Toledo College of Medicine, Toledo, OH. Contact LGK Lauren.Koch2@UToledo.Edu or SLB
447 britttons@umich.edu for information on the exercise rat models. The Russian study was supported in part by
448 grant from the Russian Science Foundation (Grant No. 17-15-01436: "Comprehensive analysis of the
449 contribution of genetic, epigenetic and environmental factors in the individual variability of the composition
450 of human muscle fibers"; DNA sample collection, genotyping and determination of muscle fiber composition
451 of Russian subjects).

452

453 References

- 454 1. Agrawal PB, Pierson CR, Joshi M, Liu X, Ravenscroft G, Moghadaszadeh B, Talabere T, Viola M, Swanson
455 LC, Talim B, Yau KS, Allcock RJNN, Laing NG, Perrella MA, Haliloğlu G, Talim B, Yau KS, Allcock RJNN,
456 Laing NG, Perrella MA, Beggs AH. SPEG Interacts with Myotubularin, and Its Deficiency Causes
457 Centronuclear Myopathy with Dilated Cardiomyopathy. *Am J Hum Genet* 95: 218–226, 2014.
- 458 2. Ahmetov I, Kulemin N, Popov D, Naumov V, Akimov E, Bravy Y, Egorova E, Galeeva A, Generozov E,
459 Kostryukova E, Larin A, Mustafina L, Ospanova E, Pavlenko A, Starnes L, Żmijewski P, Alexeev D,
460 Vinogradova O, Govorun V. Genome-wide association study identifies three novel genetic markers
461 associated with elite endurance performance. *Biol Sport* 32: 3–9, 2015.
- 462 3. Alswied A, Parekh AB. Ca²⁺ Influx through Store-operated Calcium Channels Replenishes the
463 Functional Phosphatidylinositol 4,5-Bisphosphate Pool Used by Cysteinyl Leukotriene Type I
464 Receptors. *J Biol Chem* 290: 29555–29566, 2015.
- 465 4. Bouchard C, An P, Rice T, Skinner JS, Wilmore JH, Gagnon J, Pérusse L, Leon AS, Rao DC. Familial
466 aggregation of VO₂(max) response to exercise training: results from the HERITAGE Family Study. *J*
467 *Appl Physiol* 87: 1003–8, 1999.
- 468 5. Bouchard C, Rankinen T. Individual differences in response to regular physical activity. In: *Medicine*
469 *and Science in Sports and Exercise*. 2001.
- 470 6. Bouchard C, Rankinen T, Chagnon YC, Rice T, Pérusse L, Gagnon J, Borecki I, An P, Leon AS, Skinner JS,
471 Wilmore JH, Province M, Rao DC. Genomic scan for maximal oxygen uptake and its response to
472 training in the HERITAGE Family Study. *J Appl Physiol* 88: 551–9, 2000.
- 473 7. Boulé NG, Weisnagel SJ, Lakka TA, Tremblay A, Bergman RN, Rankinen T, Leon AS, Skinner JS, Wilmore
474 JH, Rao DC, Bouchard C, HERITAGE Family Study. Effects of exercise training on glucose homeostasis:
475 the HERITAGE Family Study. *Diabetes Care* 28: 108–14, 2005.
- 476 8. Burniston JG, Connolly J, Kainulainen H, Britton SL, Koch LG. Label-free profiling of skeletal muscle
477 using high-definition mass spectrometry. *Proteomics* (2014). doi: 10.1002/pmic.201400118.
- 478 9. Burniston JG, Kenyani J, Gray D, Guadagnin E, Jarman IH, Cobley JN, Cuthbertson DJ, Chen Y-W,
479 Wastling JM, Lisboa PJ, Koch LG, Britton SL. Conditional independence mapping of DIGE data reveals
480 PDIA3 protein species as key nodes associated with muscle aerobic capacity. *J Proteomics* 106: 230–
481 45, 2014.
- 482 10. Burniston JG, Kenyani J, Wastling JM, Burant CFCF, Qi NRNR, Koch LGLG, Britton SLSL. Proteomic
483 analysis reveals perturbed energy metabolism and elevated oxidative stress in hearts of rats with
484 inborn low aerobic capacity. *Proteomics* 11: 3369–3379, 2011.

- 485 11. **Dimopoulou I, Tsintzas OK, Daganou M, Cokkinos D V., Tzelepis GE.** Contribution of Lung Function to
486 Exercise Capacity in Patients with Chronic Heart Failure. *Respiration* 66: 144–149, 1999.
- 487 12. **Drexler HCA, Ruhs A, Konzer A, Mendler L, Bruckskotten M, Looso M, Günther S, Boettger T, Krüger M,**
488 **Braun T.** On marathons and Sprints: an integrated quantitative proteomics and transcriptomics
489 analysis of differences between slow and fast muscle fibers. *Mol Cell Proteomics* 11: M111.010801,
490 2012.
- 491 13. **Edwards JN, Friedrich O, Cully TR, von Wegner F, Murphy RM, Launikonis BS.** Upregulation of
492 store-operated Ca²⁺ entry in dystrophic mdx mouse muscle. *Am J Physiol Physiol* 299: C42–C50,
493 2010.
- 494 14. **Fraysse B, Guicheney P, Bitoun M.** Calcium homeostasis alterations in a mouse model of the Dynamin
495 2-related centronuclear myopathy. *Biol Open* 5: 1691–1696, 2016.
- 496 15. **Frings S, Seifert R, Godde M, Kaupp UB.** Profoundly different calcium permeation and blockage
497 determine the specific function of distinct cyclic nucleotide-gated channels. *Neuron* 15: 169–179,
498 1995.
- 499 16. **Grundey SM, Brewer HB, Cleeman JI, Smith SC, Lenfant C.** Definition of Metabolic Syndrome. *Circulation*
500 109: 433–438, 2004.
- 501 17. **GTEx Consortium, Laboratory DA & Coordinating C (LDACC)—Analysis WG, Statistical Methods**
502 **groups—Analysis Working Group, Enhancing GTEx (eGTEx) groups, NIH Common Fund, NIH/NCI,**
503 **NIH/NHGRI, NIH/NIMH, NIH/NIDA, Biospecimen Collection Source Site—NDRI, Biospecimen Collection**
504 **Source Site—RPCI, Biospecimen Core Resource—VARI, Brain Bank Repository—University of Miami**
505 **Brain Endowment Bank, Leidos Biomedical—Project Management, ELSI Study, Genome Browser Data**
506 **Integration & Visualization—EBI, Genome Browser Data Integration & Visualization—UCSC Genomics**
507 **Institute U of CSC, Lead analysts:, Laboratory DA & Coordinating C (LDACC):, NIH program**
508 **management:, Biospecimen collection:, Pathology:, eQTL manuscript working group:, Battle A, Brown**
509 **CD, Engelhardt BE, Montgomery SB.** Genetic effects on gene expression across human tissues. *Nature*
510 550: 204–213, 2017.
- 511 18. **Guo H, Isserlin R, Emili A, Burniston JG.** Exercise-responsive phosphoproteins in the heart. *J Mol Cell*
512 *Cardiol* 111: 61–68, 2017.
- 513 19. **Hajóczky G, Robb-Gaspers LD, Seitz MB, Thomas AP.** Decoding of cytosolic calcium oscillations in the
514 mitochondria. *Cell* 82: 415–424, 1995.
- 515 20. **Holloway K V, Gorman MO, Woods P, Morton JP, Evans L, Cable NTNT, Goldspink DF, Burniston JG.**
516 Proteomic investigation of changes in human vastus lateralis muscle in response to interval-exercise
517 training. *Proteomics* 9: 5155–5174, 2009.

- 518 21. Hsieh CM, Fukumoto S, Layne MD, Maemura K, Charles H, Patel A, Perrella MA, Lee ME. Striated
519 muscle preferentially expressed genes α and β are two serine/threonine protein kinases derived from
520 the same gene as the aortic preferentially expressed gene-1. *J Biol Chem* 275: 36966–36973, 2000.
- 521 22. Hubal MJ, Gordish-Dressman H, Thompson PD, Price TB, Hoffman EP, Angelopoulos TJ, Gordon PM,
522 Moyna NM, Pescatello LS, Visich PS, Zoeller RF, Seip RL, Clarkson PM. Variability in muscle size and
523 strength gain after unilateral resistance training. *Med Sci Sports Exerc* 37: 964–72, 2005.
- 524 23. Huntoon V, Widrick JJ, Sanchez C, Rosen SM, Kutchukian C, Cao S, Pierson CR, Liu X, Perrella MA, Beggs
525 AH, Jacquemond V, Agrawal PB. SPEG-deficient skeletal muscles exhibit abnormal triad and defective
526 calcium handling. *Hum Mol Genet* 27: 1608–1617, 2018.
- 527 24. Ivarsson N, Mattsson CM, Cheng AJ, Bruton JD, Ekblom B, Lanner JT, Westerblad H. SR Ca²⁺ leak in
528 skeletal muscle fibers acts as an intracellular signal to increase fatigue resistance. *J Gen Physiol* 151:
529 567–577, 2019.
- 530 25. Johnson ML, Irving BA, Lanza IR, Vendelbo MH, Konopka AR, Robinson MM, Henderson GC, Klaus KA,
531 Morse DM, Heppelmann C, Bergen HR, Dasari S, Schimke JM, Jakaitis DR, Nair KS. Differential Effect of
532 Endurance Training on Mitochondrial Protein Damage, Degradation, and Acetylation in the Context of
533 Aging. *Journals Gerontol - Ser A Biol Sci Med Sci* 70: 1386–1393, 2015.
- 534 26. Kapfhamer D, King I, Zou ME, Lim JP, Heberlein U, Wolf FW. JNK Pathway Activation Is Controlled by
535 Tao/TAOK3 to Modulate Ethanol Sensitivity. *PLoS One* 7: e50594, 2012.
- 536 27. Keinan N, Pahima H, Ben-Hail D, Shoshan-Barmatz V. The role of calcium in VDAC1 oligomerization and
537 mitochondria-mediated apoptosis. *Biochim Biophys Acta - Mol Cell Res* 1833: 1745–1754, 2013.
- 538 28. Keller P, Vollaard NBJ, Gustafsson T, Gallagher JJ, Sundberg CJ, Rankinen T, Britton SL, Bouchard C, Koch
539 LG, Timmons JA. A transcriptional map of the impact of endurance exercise training on skeletal
540 muscle phenotype. *J Appl Physiol* 110: 46–59, 2011.
- 541 29. Kichaev G, Bhatia G, Loh P-R, Gazal S, Burch K, Freund MK, Schoech A, Pasaniuc B, Price AL. Leveraging
542 Polygenic Functional Enrichment to Improve GWAS Power. *Am J Hum Genet* 104: 65–75, 2019.
- 543 30. Koch LG, Kemi OJ, Qi N, Leng SX, Bijma P, Gilligan LJ, Wilkinson JE, Wisløff H, Høydal MA, Rolim N,
544 Abadir PM, Van Grevenhof EM, Smith GL, Burant CF, Ellingsen Ø, Britton SL, Wisløff U. Intrinsic aerobic
545 capacity sets a divide for aging and longevity. *Circ Res* 109: 1162–1172, 2011.
- 546 31. Koch LG, Pollott GE, Britton SL. Selectively bred rat model system for low and high response to
547 exercise training. *Physiol Genomics* 45: 606–614, 2013.
- 548 32. Lessard SJ, MacDonald TL, Pathak P, Han MS, Coffey VG, Edge J, Rivas DA, Hirshman MF, Davis RJ,
549 Goodyear LJ. JNK regulates muscle remodeling via myostatin/SMAD inhibition. *Nat Commun* 9: 3030,
550 2018.

- 551 33. **Lessard SJ, Rivas DA, Alves-Wagner AB, Hirshman MF, Gallagher IJ, Constantin-Teodosiu D, Atkins R,**
552 **Greenhaff PL, Qi NR, Gustafsson T, Fielding RA, Timmons JA, Britton SL, Koch LG, Goodyear LJ.**
553 Resistance to aerobic exercise training causes metabolic dysfunction and reveals novel
554 exercise-regulated signaling networks. *Diabetes* 62: 2717–2727, 2013.
- 555 34. **Levin Y, Hradetzky E, Bahn S.** Quantification of proteins using data-independent analysis (MS E) in
556 simple and complex samples: A systematic evaluation. *Proteomics* 11: 3273–3287, 2011.
- 557 35. **Li GZ, Vissers JPC, Silva JC, Golick D, Gorenstein M V, Geromanos SJ.** Database searching and
558 accounting of multiplexed precursor and product ion spectra from the data independent analysis of
559 simple and complex peptide mixtures. *Proteomics* 9: 1696–1719, 2009.
- 560 36. **Litjens T, Nguyen T, Castro J, Aromataris EC, Jones L, Barritt GJ, Rychkov GY.** Phospholipase C- γ 1 is
561 required for the activation of store-operated Ca²⁺ channels in liver cells. *Biochem J* 405: 269–276,
562 2007.
- 563 37. **Marton O, Koltai E, Takeda M, Koch LG, Britton SL, Davies KJA, Boldogh I, Radak Z.** Mitochondrial
564 biogenesis-associated factors underlie the magnitude of response to aerobic endurance training in
565 rats. *Pflügers Arch - Eur J Physiol* 467: 779–788, 2015.
- 566 38. **Matecki S, Dridi H, Jung B, Saint N, Reiken SR, Scheuermann V, Mrozek S, Santulli G, Umanskaya A,**
567 **Petrof BJ, Jaber S, Marks AR, Lacampagne A.** Leaky ryanodine receptors contribute to diaphragmatic
568 weakness during mechanical ventilation. *Proc Natl Acad Sci* 113: 9069–9074, 2016.
- 569 39. **Murgia M, Toniolo L, Nagaraj N, Ciciliot S, Vindigni V, Schiaffino S, Reggiani C, Mann M.** Single Muscle
570 Fiber Proteomics Reveals Fiber-Type-Specific Features of Human Muscle Aging. *Cell Rep* 19: 2396–
571 2409, 2017.
- 572 40. **Myers J, Kaykha A, George S, Abella J, Zaheer N, Lear S, Yamazaki T, Froelicher V.** Fitness versus
573 physical activity patterns in predicting mortality in men. *Am J Med* 117: 912–918, 2004.
- 574 41. **Pan Z, Brotto M, Ma J.** Store-operated Ca²⁺ entry in muscle physiology and diseases. *BMB Rep.*: 2014.
- 575 42. **Pickering C, Suraci B, Semenova EA, Boulygina EA, Kostyukova ES, Kulemin NA, Borisov O V., Khabibova**
576 **SA, Larin AK, Pavlenko A V., Lyubaeva E V., Popov D V., Lysenko EA, Vepkhvadze TF, Lednev EM,**
577 **Leońska-Duniec A, Pająk B, Chycki J, Moska W, Lulińska-Kuklik E, Dornowski M, Maszczyk A, Bradley B,**
578 **Kana-ah A, Ciężczyk P, Generozov E V., Ahmetov II.** A Genome-Wide Association Study of Sprint
579 Performance in Elite Youth Football Players. *J Strength Cond Res* 33: 2344–2351, 2019.
- 580 43. **Potts GK, McNally RM, Blanco R, You J-S, Hebert AS, Westphall MS, Coon JJ, Hornberger TA.** A map of
581 the phosphoproteomic alterations that occur after a bout of maximal-intensity contractions. *J Physiol*
582 595: 5209–5226, 2017.
- 583 44. **Prakriya M, Lewis RS.** Store-Operated Calcium Channels. *Physiol Rev* 95: 1383–436, 2015.

- 584 45. **Quan C, Li M, Du Q, Chen Q, Wang H, Campbell D, Fang L, Xue B, MacKintosh C, Gao X, Ouyang K, Wang**
585 **HY, Chen S.** SPEG Controls Calcium Reuptake Into the Sarcoplasmic Reticulum Through Regulating
586 SERCA2a by Its Second Kinase-Domain. *Circ Res* 124: 712–726, 2019.
- 587 46. **Quick AP, Wang Q, Philippen LE, Barreto-Torres G, Chiang DY, Beavers D, Wang G, Khalid M, Reynolds**
588 **JO, Campbell HM, Showell J, McCauley MD, Scholten A, Wehrens XHT.** SPEG (Striated Muscle
589 Preferentially Expressed Protein Kinase) Is Essential for Cardiac Function by Regulating Junctional
590 Membrane Complex Activity. *Circ Res* 120: 110–119, 2017.
- 591 47. **Rivas DA, Lessard SJ, Saito M, Friedhuber AM, Koch LG, Britton SL, Yaspelkis BB, Hawley JA.** Low
592 intrinsic running capacity is associated with reduced skeletal muscle substrate oxidation and lower
593 mitochondrial content in white skeletal muscle. *Am J Physiol Integr Comp Physiol* 300: R835–R843,
594 2011.
- 595 48. **Ross R, Goodpaster BH, Koch LG, Sarzynski MA, Kohrt WM, Johannsen NM, Skinner JS, Castro A, Irving**
596 **BA, Noland RC, Sparks LM, Spielmann G, Day AG, Pitsch W, Hopkins WG, Bouchard C.** Precision exercise
597 medicine: Understanding exercise response variability. *Br J Sports Med* 53: 1141–1153, 2019.
- 598 49. **Shathasivam P, Kollara A, Ringuette MJ, Virtanen C, Wrana JL, Brown TJ.** Human ortholog of Drosophila
599 Melted impedes SMAD2 release from TGF- β receptor I to inhibit TGF- β signaling. *Proc Natl Acad Sci*
600 112: E3000–E3009, 2015.
- 601 50. **Silva Cornachione A, Cação Oliveira Benedi P, Cristina Polizello J, César Carvalho L, Cláudia**
602 **Mattiello-Sverzut A.** Characterization of Fiber Types in Different Muscles of the Hindlimb in Female
603 Weanling and Adult Wistar Rats. *ACTA Histochem Cytochem* 44: 43–50, 2011.
- 604 51. **Silva JC, Gorenstein M V, Li G, Vissers JPC, Geromanos SJ.** Absolute Quantification of Proteins by LCMS
605 E. *Mol Cell Proteomics* 5: 144–156, 2006.
- 606 52. **Sollanek KJKJ, Burniston JGJG, Kavazis ANAN, Morton ABAB, Wiggs MP, Ahn B, Smuder AJAJ, Powers**
607 **SKSK, Wiggs P, Ahn B, Smuder AJAJ, Powers SKSK.** Global Proteome Changes in the Rat Diaphragm
608 Induced by Endurance Exercise Training. *PLoS One* 12: 1–21, 2017.
- 609 53. **Storey JD, Tibshirani R.** Statistical significance for genomewide studies. *Proc Natl Acad Sci U S A* 100:
610 9440–5, 2003.
- 611 54. **Sutter S, Raeker M, Borisov A, Russell M.** Orthologous relationship of obscurin and Unc-89: phylogeny
612 of a novel family of tandem myosin light chain kinases. *Dev Genes Evol* 214: 352–359, 2004.
- 613 55. **Tassi E, Biesova Z, Di Fiore PP, Gutkind JS, Wong WT.** Human JIK, a Novel Member of the STE20 Kinase
614 Family That Inhibits JNK and Is Negatively Regulated by Epidermal Growth Factor. *J Biol Chem* 274:
615 33287–33295, 1999.
- 616 56. **Warburton DER, Nicol CW, Bredin SSD.** Health benefits of physical activity: the evidence. 174: 801–

- 617 809, 2006.
- 618 57. **Wisloff U, Wisløff U, Najjar SM, Ellingsen Ø, Haram PM, Swoap S, Al-Share Q, Fernström M, Rezaei K,**
619 **Lee SJ, Koch LG, Britton SL.** Cardiovascular Risk Factors Emerge After Artificial Selection for Low
620 Aerobic Capacity. *Science (80-)* 307: 418–420, 2005.
- 621 58. **Wu S, Moore TM, Brough GH, Whitt SR, Chinkers M, Li M, Stevens T.** Cyclic Nucleotide-gated Channels
622 Mediate Membrane Depolarization following Activation of Store-operated Calcium Entry in
623 Endothelial Cells. *J Biol Chem* 275: 18887–18896, 2000.
- 624 59. **Yi Z, Bowen BP, Hwang H, Jenkinson CPL, Coletta DK, Lefort N, Bajaj M, Kashyap S, Berria R, De Filippis**
625 **EA, Mandarino LJ.** Global Relationship between the Proteome and Transcriptome of Human Skeletal
626 Muscle. *J Proteome Res* 7: 3230–3241, 2008.
- 627

628 **Figure 1 – Differential analysis of HDMS^E data**

629 Volcano plot presenting the log₂ fold-difference in abundance between HRT versus LRT gastrocnemius
630 and the statistical significance determined by one-way ANOVA (n=5, per group). Proteins that were
631 statistically different (P<0.05) and had a false discovery rate <1 % are highlighted in red. Proteins that
632 exhibit a >1-fold difference in abundance are annotated by UniProt protein identifiers.

633 **Figure 2 – Enzymes of the glycolytic pathway are more abundant in LRT gastrocnemius**

634 (A) Heat map of 76 proteins that differed significantly (P<0.05, q<0.01) in abundance between HRT
635 and LRT gastrocnemius (n = 5, per group). LRT muscle exhibited significant enrichment of proteins
636 associated with the KEGG metabolic pathways glycolysis and gluconeogenesis. (B) Twelve enzymes
637 involved in glycogen/glucose metabolism were more abundant in LRT muscle.

638 **Figure 3 – SPEG rs7564856 G allele frequency is greater in international-level endurance athletes**

639 Genetic association studies in Russian international-level athletes of Caucasian Eastern European
640 descent, stratified into endurance athletes (n = 258) and power athletes (n=126). The frequency of
641 the G allele of rs7564856 reported to be associated with increased expression of the *SPEG* gene was
642 significantly (P = 0.009) greater in endurance compared to power athletes.

Table 1 – Proteins more abundant in HRT gastrocnemius

Description	Accession	Score	Peptides	Delta	P value
Striated muscle-specific serine/threonine-protein kinase	Q63638	109	18 (4)	2.64	1.44E-03
Nuclear autoantigenic sperm protein	Q66HD3	44	7 (3)	2.35	2.1E-04
1-phosphatidylinositol-4,5-bisphosphate phosphodiesterase gamma-1	P10686	57	9 (4)	1.72	1.3E-04
ATP synthase protein 8	P11608	24	4 (3)	1.67	4.85E-09
cGMP-gated cation channel alpha-1	Q62927	83	11 (3)	1.53	1.81E-03
Stromal interaction molecule 1	P84903	38	6 (4)	1.42	7.78E-06
Ras-related protein Rab-35	Q5U316	106	14 (4)	1.4	5.3E-04
Alcohol dehydrogenase [NADP+]	P51635	80	13 (6)	1.28	1.1E-04
10 kDa heat shock protein, mitochondrial	P26772	65	10 (7)	1.27	9.1E-04
Inositol monophosphatase	P97697	123	18 (10)	1.26	1.9E-04
Platelet glycoprotein 4	Q07969	28	5 (4)	1.25	7.7E-04
Superoxide dismutase [Mn], mitochondrial	P07895	51	10 (6)	1.21	4.8E-04
Cytochrome c oxidase subunit 6C-2	P11951	69	11 (5)	1.15	9.4E-04

Protein description and Accession relate to the Swiss-Prot database entry identified from MSe searches performed in TransOmics via GLPS. Delta is the fold difference relative to LRT. Values are reported for proteins quantified using 3 or more peptides and exhibiting significant ($P < 0.05$) differences in abundance at a false discovery rate of $< 1\%$.

Table 2 – Proteins more abundant in LRT gastrocnemius

Description	Accession	Score	Peptides	Delta	P value
Membrane/ cytoskeletal/ vesicle/ microtubule					
Ras-related protein Rab-27B	Q99P74	38	6 (3)	1.96	1.25E-04
Ras-related protein Rab-9A	Q99P75	43	6 (6)	1.72	2.08E-04
Tripartite motif-containing protein 72	A0JPQ4	261	28 (22)	1.56	3.37E-05
Signal-induced proliferation-associated 1-like protein 1	O35412	327	52 (21)	1.41	1.24E-04
Growth arrest-specific protein 8	Q499U4	51	8 (6)	1.38	9.09E-09
Myosin-1e	Q63356	96	16 (6)	1.37	8.65E-07
Potassium voltage-gated channel subfamily A member 5	P19024	65	12 (7)	1.25	1.03E-05
Protocadherin Fat 3	Q8R508	279	52 (17)	1.23	1.84E-04
Annexin A4	P55260	169	25 (14)	1.16	5.92E-05
Cofilin-1	P45592	104	15 (8)	1.15	6.96E-04
Annexin A6	P48037	523	67 (44)	1.12	2.36E-04
Dynein heavy chain 12, axonemal	Q923J6	797	132 (57)	1.11	6.2E-05

Microtubule-associated protein 1B	P15205	188	30 (15)	1.11	6.94E-04
Glucose metabolic processes					
Glyceraldehyde-3-phosphate dehydrogenase	P04797	473	62 (34)	1.77	1.58E-03
L-lactate dehydrogenase A chain	P04642	450	78 (40)	1.47	1.56E-06
Fatty acid-binding protein, epidermal	P55053	34	4 (3)	1.38	1.09E-03
Glucose-6-phosphate isomerase	Q6P6V0	485	65 (46)	1.37	5.45E-08
Glycogen phosphorylase, brain form (Fragment)	P53534	631	83 (23)	1.34	7.83E-05
6-phosphofructokinase, muscle type	P47858	477	63 (35)	1.31	1.14E-03
Glycogen phosphorylase, muscle form	P09812	1275	188 (104)	1.28	3.39E-06
Fructose-bisphosphate aldolase A	P05065	554	76 (43)	1.28	1.02E-05
Beta-enolase	P15429	687	101 (26)	1.27	7.6E-04
Glycogen [starch] synthase, muscle	A2RRU1	284	41 (28)	1.26	2.7E-05
Triosephosphate isomerase	P48500	368	58 (43)	1.25	1.13E-05
Phosphoglycerate kinase 1	P16617	512	79 (54)	1.25	4.55E-05
Aldose reductase	P07943	209	30 (22)	1.24	5.43E-05
Phosphoglycerate mutase 2	P16290	290	40 (15)	1.24	8.11E-05

Mitochondrion					
Acyl-CoA synthetase family member 2, mitochondrial	Q499N5	36	7 (5)	1.41	1.69E-04
Trans-2,3-enoyl-CoA reductase	Q64232	41	5 (3)	1.37	1.35E-03
NADP-dependent malic enzyme	P13697	70	11 (7)	1.3	1.59E-03
Citrate synthase, mitochondrial	Q8VHF5	213	25 (19)	1.3	1.49E-03
Voltage-dependent anion-selective channel protein 1	Q9Z2L0	293	35 (28)	1.27	6.57E-05
ADP/ATP translocase 1	Q05962	275	35 (8)	1.21	7.6E-05
Phosphatidylethanolamine-binding protein 1	P31044	106	11 (9)	1.2	1.23E-03
NADH-ubiquinone oxidoreductase 75 kDa subunit, mitochondrial	Q66HF1	378	47 (28)	1.15	1.52E-03
Medium-chain specific acyl-CoA dehydrogenase, mitochondrial	P08503	153	23 (14)	1.1	6.77E-04
Calcium handling					
Sarcoplasmic/endoplasmic reticulum calcium ATPase 1	Q64578	1060	176 (64)	1.41	1.03E-07
Protein S100-A1	P35467	37	4 (3)	1.4	2.53E-05
Parvalbumin alpha	P02625	272	45 (31)	1.39	5.71E-06
Chaperones/ protein folding					
UDP-glucose:glycoprotein glucosyltransferase 1	Q9JLA3	138	24 (7)	1.7	1.6E-06

Alpha-1,6-mannosylglycoprotein 6-beta-N-acetylglucosaminyltransferase A	Q08834	52	9 (3)	1.35	4.46E-04
Heat shock protein HSP 90-alpha	P82995	296	45 (16)	1.31	1.45E-05
Heat shock cognate 71 kDa protein	P63018	486	52 (17)	1.28	1.56E-04
T-complex protein 1 subunit beta	Q5XIM9	64	9 (7)	1.26	1.13E-03
Peptidyl-prolyl cis-trans isomerase A	P10111	123	13 (10)	1.12	2.12E-04
Signal transduction					
RAC-beta serine/threonine-protein kinase	P47197	110	20 (9)	1.39	4.53E-04
Calcium/calmodulin-dependent protein kinase type II beta chain	P08413	63	10 (4)	1.29	1.08E-04
14-3-3 protein epsilon	P62260	202	25 (15)	1.14	2.42E-04
Cell Stress					
Glutathione S-transferase Mu 2	P08010	337	37 (12)	1.5	3.08E-06
Macrophage migration inhibitory factor	P30904	36	7 (7)	1.17	2.16E-04
Dual oxidase 1	Q8CIY2	72	14 (4)	1.15	6.68E-05
Skeletal muscle-specific					
Carbonic anhydrase 3	P14141	249	43 (31)	1.26	1.43E-03
Creatine kinase M-type	P00564	549	94 (58)	1.21	5.66E-04

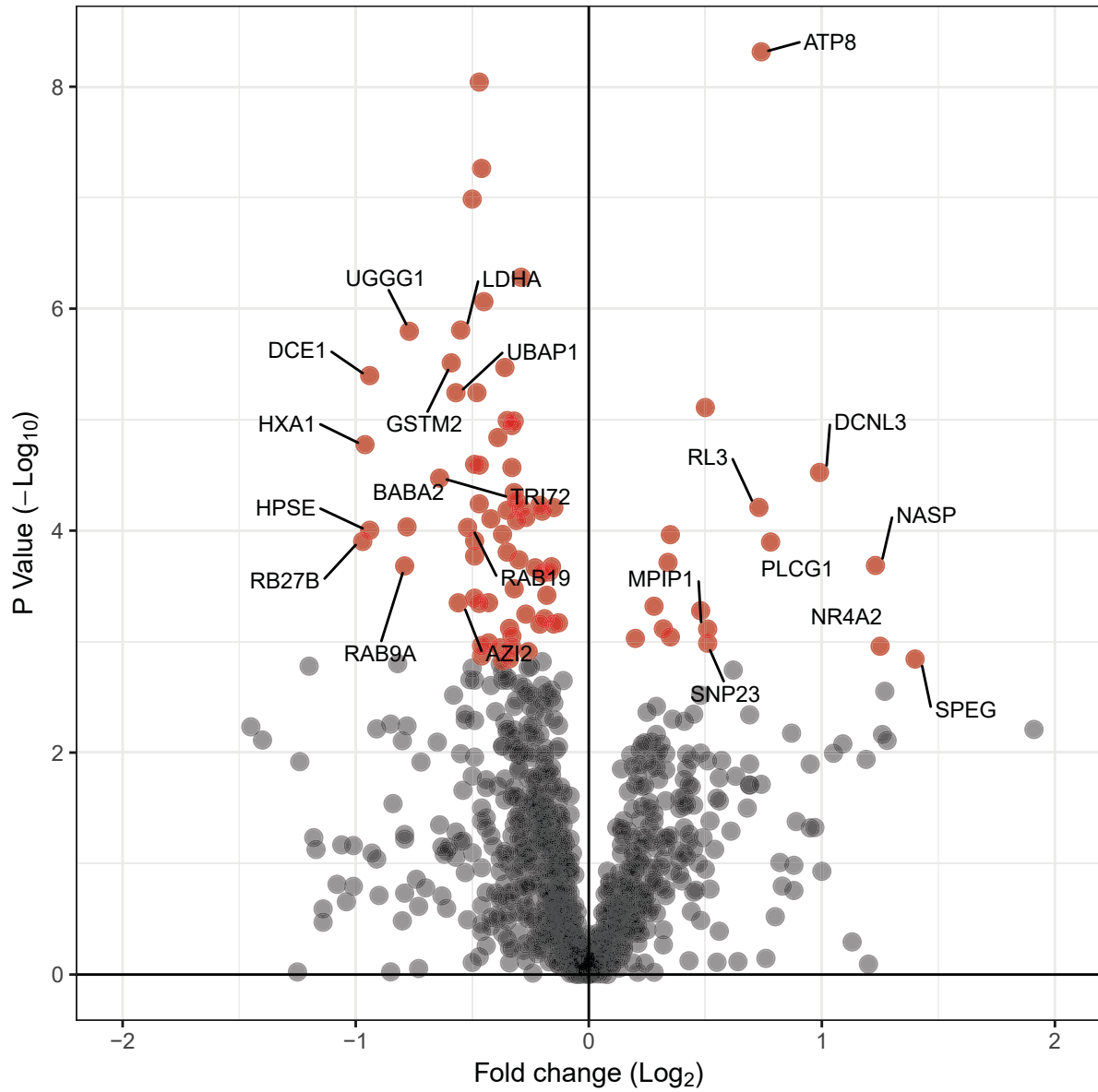
Four and a half LIM domains protein 1	Q9WUH4	229	30 (23)	1.19	1.68E-03
Post-transcriptional processing					
Protein mago nashi homolog	Q27W02	67	9 (3)	1.42	1.73E-03
Serine/threonine-protein kinase PRP4 homolog	Q5RKH1	64	12 (6)	1.29	1.87E-03
Protein turnover (ribosome/ proteasome)					
26S protease regulatory subunit 4	P62193	98	15 (6)	1.22	6.32E-05
NSFL1 cofactor p47	O35987	126	19 (12)	1.2	1.72E-03
Elongation factor 2	P05197	376	52 (34)	1.13	3.82E-04
Lipoprotein					
Apolipoprotein A-I	P04639	82	12 (7)	1.22	5.22E-07
Hemopexin	P20059	262	35 (27)	1.14	6.22E-04
Uncharacterised					
Coiled-coil domain-containing protein 146	Q66H60	110	19 (7)	1.39	5.73E-05
Coiled-coil domain-containing protein 67	Q5U3Z6	132	26 (10)	1.35	1.03E-03

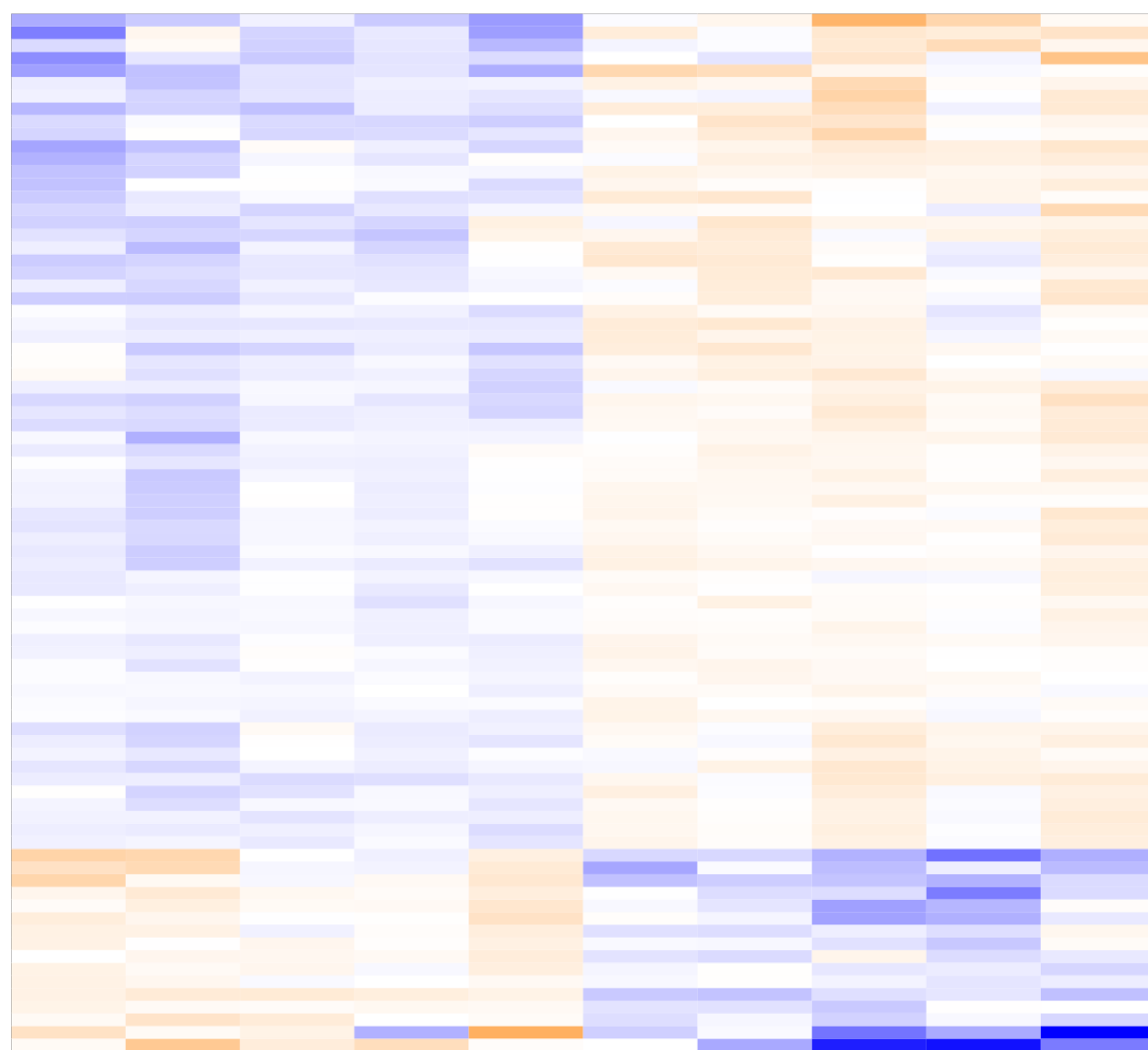
Protein description and Accession relate to the Swiss-Prot database entry identified from MS/MS searches performed in Progenesis via GLPS. Fold difference relative to HRT. Values are reported for protein quantified using 3 or more peptides and exhibiting significant differences in abundance at a false discovery rate of < 1%.

Table 3 – Putative protein-interaction partners of SPEG β in skeletal muscle

Accession	Description; protein identifier	MOWSE score	Sequence coverage (%)
C0HL12	Adhesion G protein-coupled receptor B1; AGRB1	29	3.1
Q5U2S6	Ankyrin repeat and SOCS box protein 2; ASB2	35	3.8
P70673	ATP-sensitive inward rectifier potassium channel 11; KCJ11	68	5.9
Q3KR97	Brain-specific angiogenesis inhibitor 1-associated protein 2-like protein 1; BI2L1	31	4.5
P41350	Caveolin-1; CAV1	64	32.6
P01026	Complement C3; CO3	35	4.4
Q01205	Dihydrolipoyllysine-residue succinyltransferase component of 2-oxoglutarate dehydrogenase complex, mitochondrial; ODO2	51	7.3
P39052	Dynamin-2; DYN2	36	4.5
M0R8U1	Dynein heavy chain 5, axonemal; DYH5	30	2.5
Q5U4E6	Golgin subfamily A member 4; GOGA4	40	4.6
P97636	Interleukin-18; IL18	29	13.4
O35790	N-acetylglucosaminyl-phosphatidylinositol de-N-acetylase; PIGL	34	5.2

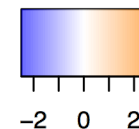
P51839	Olfactory guanylyl cyclase GC-D; GUC2D	31	0.8
Q8K4M9	Oxysterol-binding protein-related protein 1; OSBL1	30	3.5
Q505J8	Phenylalanine--tRNA ligase alpha subunit; SYFA	29	2.2
P33568	Retinoblastoma-associated protein; RB	34	1.4
Q53UA7	Serine/threonine-protein kinase TAO3; TAOK3	137	8.1
P02770	Serum albumin; ALBU	46	5.6
A4ZYQ5	Solute carrier family 2, facilitated glucose transporter member 7; GTR7	28	2.1
Q63638*	Striated muscle-specific serine/threonine-protein kinase; SPEG	68	1.1
P46462	Transitional endoplasmic reticulum ATPase; TERA	116	18.7
Q6AY56	Tubulin alpha-8 chain; TBA8	31	11.1
Q5PQS3	Ventricular zone-expressed PH domain-containing protein homolog 1; MELT	32	3.1
Q8K3Y6	Zinc finger CCCH-type antiviral protein 1; ZCCHV	30	4



a

HRT

LRT

Fold change (Log₂)**b**